

## Quantum interference patterns and electron confinement on a two-dimensional metal: A scanning tunneling microscopy study

I. Brihuega,<sup>1</sup> P. Mallet,<sup>2</sup> L. Magaud,<sup>2</sup> S. Pons,<sup>2</sup> O. Custance,<sup>1</sup> J. M. Gómez-Rodríguez,<sup>1</sup> and J.-Y. Veuillen<sup>2</sup>

<sup>1</sup>*Departamento de Física de la Materia Condensada, Universidad Autónoma de Madrid, E-28049-Madrid, Spain*

<sup>2</sup>*Laboratoire d'Etude des Propriétés Electroniques des Solides (LEPES-CNRS), Boîte Postale 166, 38042 Grenoble Cedex 9, France*

(Received 29 July 2003; published 12 April 2004)

We have investigated by scanning tunneling microscopy (STM) the electronic structure of a monolayer thick metallic film grown on top of a semiconducting substrate. In this system, which should behave as a true two-dimensional metal in the vicinity of the Fermi level, we have observed standing-wave patterns at low sample bias. The analysis of the modulations of the local density of states inside elongated resonators as a function of the bias shows that we probe a dispersive surface state with downward dispersion. The present STM results are in excellent agreement with previously reported photoemission data and with our band-structure *ab initio* calculations.

DOI: 10.1103/PhysRevB.69.155407

PACS number(s): 73.20.At, 72.10.Fk, 73.22.Dj

The so-called Shockley surface state of noble-metal surfaces<sup>1</sup> has been the subject of impressive scanning tunneling microscopy (STM) studies in the last few years. Several fundamental physical phenomena could be investigated using this experimental realization of a two-dimensional (2D) electron gas: quantum interferences<sup>2,3</sup> and confinement effects,<sup>4,5</sup> lifetime of excited states,<sup>6,7</sup> interaction between adatoms mediated by the surface electrons,<sup>8,9</sup> etc. Bulk electrons, which exist in the same energy range as the surface state, generally have to be taken into account for a proper understanding of these effects. For instance, transition to bulk states reduces the efficiency of the confinement on surface structures<sup>10-12</sup> and the decay of excited electrons in the surface band can proceed via transition to bulk states.<sup>7,13,14</sup> Moreover, due to their high density, the bulk electrons should provide an efficient screening of charges in the surface region, including electrons in the surface state.<sup>7,15</sup> The situation should be radically different in the case of a monolayer (ML) thick metallic layer on top of a semiconducting substrate. In the vicinity of the Fermi level (FL), there will be no bulk states at the same energy as the states of the surface metallic film. Accordingly, scattering from surface to bulk states will not be possible in a certain energy range that depends on the value of the gap and of the Schottky barrier height. Additionally, in the surface region, the screening by the semiconducting substrate should be less efficient than in the case of a bulk metallic sample. Therefore differences are expected in the physical properties of the surface electrons between Shockley states at metal surfaces and metallic overlayers on semiconducting substrates, these latter systems being presumably closer to the true 2D case where specific effects may eventually show up.<sup>16</sup>

In this paper, we report a STM observation of quantum interferences and confinement effects on a genuine 2D metal, which consists of a monolayer of metallic silicide epitaxially grown on top of a semiconducting substrate. The system we have chosen is the 2D erbium silicide phase that forms for submonolayer coverage on the Si(111) surface. The growth,<sup>17</sup> the atomic,<sup>18</sup> and the electronic structure<sup>19,20</sup> of this metallic surface layer are well known from previous experimental studies. The band structure consists of two bands

crossing the FL. The first one is almost fully occupied, it disperses downwards from the center of the surface Brillouin zone (SBZ) and gives rise to a hole pocket at  $\Gamma$ . The second one is almost fully empty, it disperses upwards from the  $M$  point at the SBZ boundary. The atomic structure consists of an Er monolayer occupying  $T4$  sites on the Si(111) surface, and covered by a relaxed Si(111) bilayer rotated by  $180^\circ$ . The FL of the silicide layer is located close to the conduction-band minimum in the monolayer range.<sup>21</sup> As a result, the electron states of the 2D silicide with energies between  $\approx 0.08$  eV above and 1.0 eV below the FL are located in the total gap of the silicon substrate. Although the observation of quantum interferences and confinement effects by STM on metallic layers on top of semiconducting substrates has already been reported,<sup>22,23</sup> in one case,<sup>22</sup> the metallic layer was the accumulation gas at the surface of InAs(111)A, which gives an electron gas with a much lower density than the one investigated here, while in Ref. 23, standing-wave patterns were observed for the system Ag/Si(111), but the dispersion deduced from the STM data was at variance with previous results on the same system, and measurements were not possible close to the FL.

The samples have been prepared according to the recipe given in Refs. 17 and 18. Between 0.5 and 1 ML Er [referred to the Si(111)  $1 \times 1$  atomic density] was deposited on clean Si(111)  $7 \times 7$  surfaces held at room temperature. The sample was then annealed at about  $400^\circ\text{C}$  for 15 min in order to promote the growth of the 2D silicide, and then transferred to the microscope and cooled down to typically 40 K. We have obtained similar results using both  $n$ -type ( $\rho \approx 1 \Omega \text{ cm}$ ) and highly doped  $p$ -type ( $\rho \approx 0.015 \Omega \text{ cm}$ ) Si substrates. The STM setup is briefly presented in Ref. 24. Conductance images on linear nano-objects (resonators) were recorded using a current imaging tunneling spectroscopy (CITS) technique:<sup>25</sup> an  $I(V)$  characteristic is acquired (in open feedback loop mode) at each point of a topography (recorded in closed feedback loop mode). The conductance ( $dI/dV$ ) images are constructed by numerically differentiating the  $I(V)$  curves. The sample bias for the topographic image was chosen high enough to avoid the contribution of

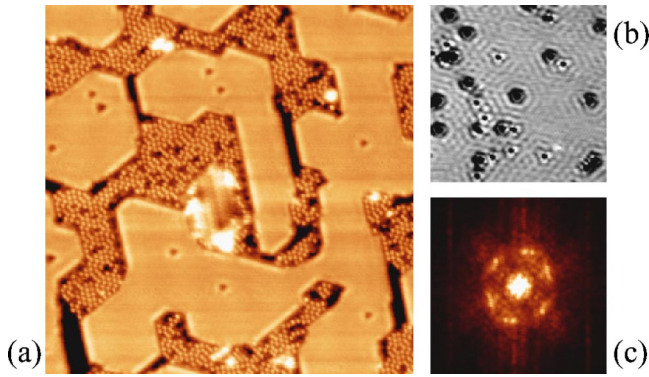


FIG. 1. (Color online) (a) Constant current image of a 0.5 ML Er deposit taken at 42 K. Size of the image,  $50 \times 50 \text{ nm}^2$ ; sample bias, +1.0 V; tunneling current, 1.0 nA. (b)  $40 \times 40 \text{ nm}^2$  constant current image of a 1.0 ML deposit taken at 40 K. Sample bias, -3 mV; tunneling current, 0.1 nA. (c) Fourier transform of (b). Size of the frame:  $10.1 \times 10.1 \text{ nm}^{-2}$  (the actual wave-vector values have been divided by a factor of 2).

the standing-wave patterns inside the resonators to the topographic image.<sup>12,26</sup> The conductance maps obtained in this way for different sample voltages  $V$  are closely related to the spatial variations of the sample local density of states (LDOS) at energies  $eV$ , at least for low sample biases.<sup>27</sup>

Figure 1(a) shows the typical topography of a sample for a deposit of 0.5 ML of Er. In this high bias image (+1.0 V), one observes flat and featureless areas (except for some triangular defects), limited by straight edges. These structures are ascribed to islands of the 2D silicide phase.<sup>17</sup> For coverages higher than 0.5 ML, the 2D silicide islands are generally connected. Surrounding these structures are areas of bare Si showing small patches with different reconstructions, as well as Er induced reconstructed phases. When the sample bias is decreased to lower values, the surface of the 2D silicide islands shows a significant corrugation in constant current images. This is clear from Fig. 1(b), taken at -3 mV on an almost complete silicide layer. The triangular defects are surrounded by modulations whose amplitude is of the order of  $0.07 \text{ \AA}$ . These modulations are quite similar to the standing-wave patterns observed at low bias on noble-metal (111) surfaces,<sup>2,28</sup> which are due to the scattering of surface-state electrons by defects. In the latter case, it has been shown that the Fourier transform (FT) of the low bias constant current images gives an image of the Fermi surface of the surface state. The FT of the image of Fig. 1(b) is displayed in Fig. 1(c). It shows six elongated spots essentially equidistant from the center. The average distance of the six spots to the center leads to a “Fermi wave vector”:<sup>28</sup>  $k_F \approx 0.19 \text{ \AA}^{-1}$ . Extrapolations of available photoemission data<sup>19,20</sup> give a value for the actual Fermi wave vector of the almost fully occupied band of the order of  $0.15\text{--}0.20 \text{ \AA}^{-1}$  (averaged along  $\Gamma K$  and  $\Gamma M$ ). This is the first indication that the modulations of Fig. 1(b) originate from electrons in this surface-state band. The fact that we do not observe the full Fermi surface of the surface band is due to the triangular shape of the defects that moreover have a finite size.

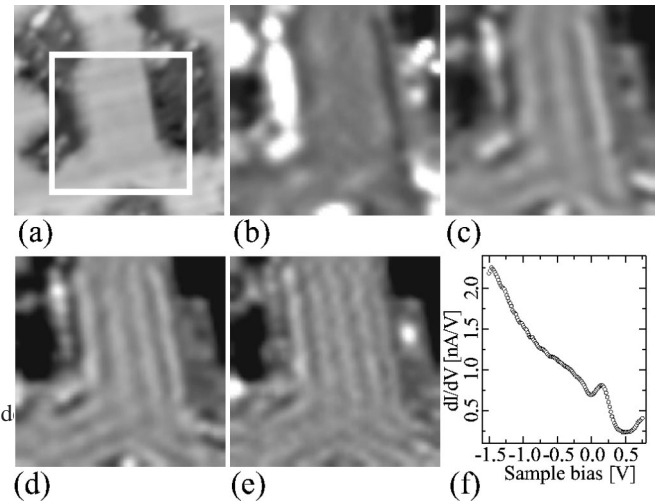


FIG. 2. (a) Constant current image of a 0.6 ML deposit taken at 40 K. Size of the image,  $16.9 \times 16.9 \text{ nm}^2$ ; sample bias, -1.5 V; tunneling current, 1.0 nA. (b)–(e) conductance ( $dI/dV$ ) images of the area marked by a square in (a), extracted from a CITS experiment. The sample biases are +200 mV (b), -6 mV (c), -143 mV (d) and -263 mV (e). Size of the images:  $10 \times 10 \text{ nm}^2$ . (f) Tunneling spectrum averaged over the central silicide island extracted from the same CITS experiment. The tip to sample distance was controlled at -1.5 V and 2.0 nA before collecting the spectra.

In order to demonstrate that we can actually probe by STM the surface state that disperses downwards from  $\Gamma$ , it is necessary to map its dispersion. This has been done on elongated structures such as the ones seen in Fig. 1(a), which we have considered as one-dimensional resonators. We use the confinement effect in these elongated objects to enhance the signal originating from the modulations of the LDOS. This allows us to probe states down to -500 meV from the FL. Figure 2(a) shows the overall topography for a deposit of 0.6 ML Er. A linear structure delimited by straight edges is enclosed in the square of Fig. 2(a). Its width is  $\approx 5 \text{ nm}$ . The conductance images at selected sample biases  $V$  are shown in Figs. 2(b)–2(e). From Figs. 2(c)–2(e), one can see modulations of the LDOS in the direction perpendicular to the edges of the island. The number of maxima increases with decreasing sample bias, which demonstrates that these modulations are due to a downward dispersing surface state. This is the situation opposite to the well-known case of the (111) surface of noble metal, where the Shockley state disperses upwards. This is again a strong indication that we are actually sensitive to the almost filled band that gives a hole pocket at the  $\Gamma$  point of the SBZ.<sup>19,20</sup> Indeed, for high enough positive voltages [e.g., +200 mV in Fig. 2(b)], the conductance images are almost featureless, which suggests that we are probing states above the top of this band. Spectra recorded on this island [see Fig. 2(f)]—as well as on many others, using different tips—actually show a peak around +160 meV, followed by a strong decrease of the conductance at higher voltages, which could mark the top of the surface band.

We have performed a more quantitative analysis of the LDOS modulations on linear resonators to establish that our

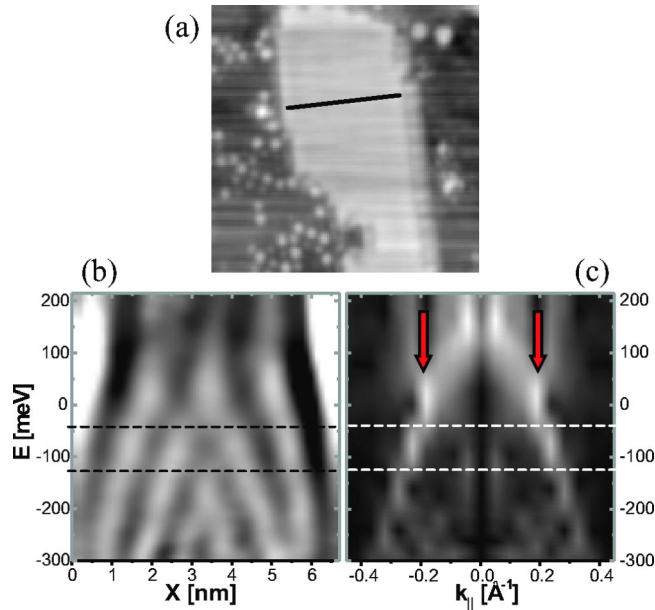


FIG. 3. (Color online) (a) Topographic image of an elongated resonator. Image size,  $15 \times 15 \text{ nm}^2$ ; sample bias,  $-500 \text{ mV}$ ; tunneling current,  $1.0 \text{ nA}$ . (b) LDOS as a function of energy  $E$  and position  $x$  along the line drawn in (a). (c) One-dimensional Fourier transform along the  $x$  axis of the data in (b). The actual wave-vector values have been divided by a factor of 2.

STM data are consistent with dispersion measured by angle-resolved photoemission spectroscopy (ARPES). For that purpose, we first create maps of the LDOS modulations vs energy across linear resonators from CITS data. An example is shown for another island in Fig. 3. Figure 3(a) is a topographic view of the resonator. Its width, measured in the upper part, is close to  $7 \text{ nm}$ . The LDOS modulations vs energy along the line drawn in Fig. 3(a) are shown in Fig. 3(b). It clearly shows the increasing number of maxima across the island with decreasing energy in a more continuous way than in Fig. 2. To retrieve the experimental dispersion from this map, we have performed a one-dimensional FT of the data along the  $x$  axis. The result is shown in Fig. 3(c) where one can see for energies below  $100 \text{ meV}$  a set of straight vertical lines (one pair is indicated by the vertical arrows) whose distance from the center increases with decreasing energy. As shown by the horizontal dashed lines in Figs. 3(b) and 3(c), one pair of vertical lines in the FT [Fig. 3(c)] is associated with a definite number  $n$  of maxima of the LDOS across the island in real space [Fig. 3(b)], i.e., each structure in the FT is associated with a specific eigenstate of order  $n$  in the transverse direction of the island. In a simple hard-wall model,<sup>29</sup> the wave vector of this state can be obtained directly from the position of the vertical line in Fig. 3(c), and the corresponding energy can be estimated roughly from the maximum of intensity of the FT along the line. In this way we obtain discrete points of the dispersion curve of the surface state. In Fig. 4 we show the data taken on six different resonators, using different tips and different substrates. Notice that the average curve passing through these points intersects the FL around  $0.20 \text{ \AA}^{-1}$ . This value is in excellent agreement with the one determined independently using low bias

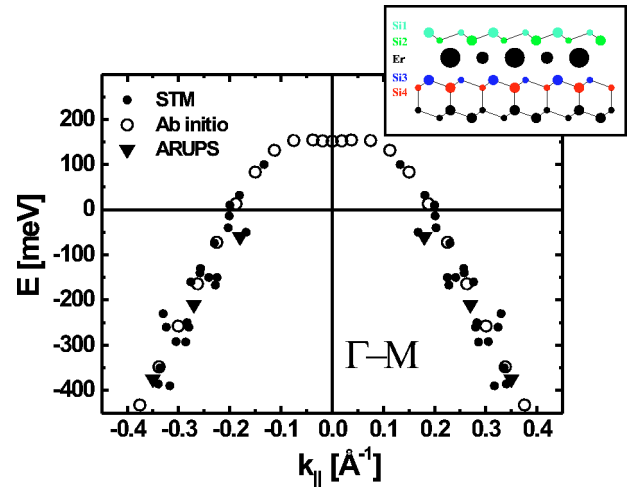


FIG. 4. (Color online) Experimental and calculated data for the dispersion of the surface state of the 2D silicide: filled dots are from STM measurements, filled triangles from ARPES (Ref. 20) and open dots from *ab initio* calculation. The inset shows a side view of the topmost layers of the sample (Ref. 18).

STM images such as the one in Fig. 1(b) ( $0.19 \text{ \AA}^{-1}$ ). Due to the orientation of the resonator edges relative to the substrate, we probe the dispersion along the  $\Gamma M$  direction of the SBZ. Data from ARPES measurements along  $\Gamma M$  on the 2D silicide are also shown in Fig. 4.<sup>20</sup> Essentially the same dispersion is found with ARPES and with STM, which definitively demonstrates that the electron state that gives rise to the LDOS modulation in the STM images is the almost filled band that disperses downward from  $\Gamma$ .

We have not found any evidence for the second surface state band that crosses the FL close to the  $M$  point in our STM experiments. This may be in part due to the fact that this state has a high- $k_{\parallel}$  wave vector in the vicinity of the FL, and therefore gives a small contribution to the STM current compared to the one of the other band with smaller wave vector. This may also come from the spatial localization of the corresponding states within the topmost atomic planes. To verify that point, we have performed *ab initio* electronic structure calculations for the case of a 2D  $\text{YSi}_2$  epitaxial layer on top of the  $\text{Si}(111)$  substrate. The yttrium silicide 2D layer has the same atomic structure as the erbium one,<sup>30</sup> but Y has no  $4f$  electrons, which facilitates the computation without affecting the band structure. Calculations are performed within the density-functional theory with Perdew and Wang generalized gradient corrections<sup>31</sup> using the VASP code.<sup>32</sup> The energy cutoff is equal to  $150 \text{ eV}$  and 100 irreducible  $k$  points are used. The supercell contains four silicon bilayers, one Y layer, the outermost (rotated) silicon bilayer, and an empty space equal to  $13.4 \text{ \AA}$ . On the other side, dangling bonds are saturated by H atoms. For the determination of the actual surface structure, all the atoms are allowed to move. After convergence, residual forces on the atoms are smaller than  $0.03 \text{ eV/\AA}$ . In agreement with experimental data on the 2D Er silicide,<sup>18</sup> we found the so-called  $T4B$  geometry to be the most stable one. Our full band-structure calculation (not shown) reproduces quite accurately the

ARPES data for the 2D Er silicide<sup>19,20</sup> in an extended energy range over the whole SBZ, as quoted above. We only show the part relevant to the present study in Fig. 4. The agreement with experimental (ARPES and STM) data is excellent. Moreover, the top of the band, located at 150 meV above the FL, corresponds quite well to the peak found at +160 mV in the tunneling spectra. From the analysis of the orbital content of the surface states, it is found that the almost empty band that disperses upwards from  $M$  is mostly localized on the Er (or Y) and Si2 planes (see inset in Fig. 4). Its weight in the outermost surface layer (Si1) is very small, which is another reason why it is not observed by STM. The band that disperses downwards from  $\Gamma$  is flat close to the SBZ center, where it has an Er (or Y)  $d_{z^2}$  and Si3  $p_z$  character. It acquires a Si1  $p_z$  (dangling-bond-like) character, and therefore a significant weight on the outermost

surface plane, for larger wave vectors (when it becomes dispersive). Since this state protrudes in vacuum, it is easily probed by STM.

In summary, we have shown that it is possible to probe successfully by STM the electronic structure of a 2D metal grown on a semiconducting substrate. A dispersive surface state is detected close to the Fermi level, in an energy range where bulk states are essentially absent. As the Shockley state of noble-metal surfaces it gives rise to quantum interferences and confinement effects. Therefore, it should be of interest for studying the fascinating phenomena formerly observed on these model metal surfaces in a situation closer to the real 2D case.

Partial financial support from Spain's MCyT Grant No. HF2001-0047 and CAM Grant No. 07N/0054/2001 is gratefully acknowledged.

- 
- <sup>1</sup>N. Memmel, Surf. Sci. Rep. **32**, 91 (1998).  
<sup>2</sup>M.F. Crommie, C.P. Lutz, and D.M. Eigler, Nature (London) **363**, 524 (1993).  
<sup>3</sup>Y. Hasegawa and Ph. Avouris, Phys. Rev. Lett. **71**, 1071 (1993).  
<sup>4</sup>M.F. Crommie, C.P. Lutz, and D.M. Eigler, Science **262**, 218 (1993).  
<sup>5</sup>J. Li, W.-D. Schneider, R. Berndt, and S. Crampin, Phys. Rev. Lett. **80**, 3332 (1998).  
<sup>6</sup>J. Li, W.-D. Schneider, R. Berndt, O.R. Bryant, and S. Crampin, Phys. Rev. Lett. **81**, 4464 (1998).  
<sup>7</sup>L. Bürgi, O. Jeandupeux, H. Brune, and K. Kern, Phys. Rev. Lett. **82**, 4516 (1999).  
<sup>8</sup>J. Repp, F. Moresco, G. Meyer, K.-H. Rieder, P. Hyldgaard, and M. Persson, Phys. Rev. Lett. **85**, 2981 (2000).  
<sup>9</sup>N. Knorr, H. Brune, M. Epple, A. Hirstein, M.A. Schneider, and K. Kern, Phys. Rev. B **65**, 115420 (2002).  
<sup>10</sup>S. Crampin, M.H. Boon, and J.E. Inglesfield, Phys. Rev. Lett. **73**, 1015 (1994); S. Crampin and O.R. Bryant, Phys. Rev. B **54**, 17367 (1996).  
<sup>11</sup>G. Hörmandinger and J.B. Pendry, Phys. Rev. B **50**, 18607 (1994).  
<sup>12</sup>L. Bürgi, O. Jeandupeux, A. Hirstein, H. Brune, and K. Kern, Phys. Rev. Lett. **81**, 5370 (1998).  
<sup>13</sup>J. Kliewer, R. Berndt, E.V. Chulkov, V.M. Silkin, P.M. Echenique, and S. Crampin, Science **288**, 1399 (2000).  
<sup>14</sup>L. Vitali, P. Wahl, M.A. Schneider, K. Kern, V.M. Silkin, E.V. Chulkov, and P.M. Echenique, Surf. Sci. **523**, L47 (2003).  
<sup>15</sup>P. Hildgaard and M. Persson, J. Phys.: Condens. Matter **12**, L13 (2000).  
<sup>16</sup>G.F. Giuliani and J.J. Quinn, Phys. Rev. B **26**, 4421 (1982); E. Zaremba, I. Nagy, and P.M. Echenique, Phys. Rev. Lett. **90**, 046801 (2003).  
<sup>17</sup>P. Wetzel, C. Pirri, G. Gewinner, S. Pelletier, P. Roge, F. Palmino, and J.-C. Labrune, Phys. Rev. B **56**, 9819 (1997).  
<sup>18</sup>P. Wetzel, C. Pirri, P. Paki, D. Bolmont, and G. Gewinner, Phys. Rev. B **47**, 3677 (1993); M. Lohmeier, W.J. Huisman, G. ter Horst, P.M. Zagwijn, E. Vlieg, C.L. Nicklin, and T.S. Turner, *ibid.* **54**, 2004 (1996).  
<sup>19</sup>L. Stauffer, A. Mharchi, C. Pirri, P. Wetzel, D. Bolmont, G. Gewinner, and C. Minot, Phys. Rev. B **47**, 10555 (1993).  
<sup>20</sup>J.-Y. Veuillen, T.A. Nguyen Tan, and D.B.B. Lollman, Surf. Sci. **293**, 86 (1993).  
<sup>21</sup>S. Vandré, T. Kalka, C. Preinesberger, and M. Dähne-Prietsch, Phys. Rev. Lett. **82**, 1927 (1999).  
<sup>22</sup>K. Kanisawa, M.J. Butcher, H. Yamaguchi, and Y. Hirayama, Phys. Rev. Lett. **86**, 3384 (2001).  
<sup>23</sup>N. Sato, S. Takeda, T. Nagao, and S. Hasegawa, Phys. Rev. B **59**, 2035 (1999).  
<sup>24</sup>S. Pons, P. Mallet, L. Magaud, and J.-Y. Veuillen, Europhys. Lett. **61**, 375 (2003).  
<sup>25</sup>R.J. Hamers, R.M. Tromp, and J.E. Demuth, Phys. Rev. Lett. **56**, 1972 (1986).  
<sup>26</sup>J. Li, W.-D. Schneider, and R. Berndt, Phys. Rev. B **56**, 7656 (1997).  
<sup>27</sup>G. Hörmandinger, Phys. Rev. B **49**, 13897 (1994).  
<sup>28</sup>L. Petersen, P.T. Sprunger, Ph. Hofmann, E. Lægsgaard, B.G. Briner, M. Doering, H.-P. Rust, A.M. Bradshaw, F. Besenbacher, and E.W. Plummer, Phys. Rev. B **57**, 6858 (1998).  
<sup>29</sup>S. Pons, P. Mallet, and J.-Y. Veuillen, Phys. Rev. B **64**, 193408 (2001).  
<sup>30</sup>C. Rogero, C. Polop, L. Magaud, J.L. Sacedon, P.L. de Andrés, and J.A. Martin-Gago, Phys. Rev. B **66**, 235421 (2002).  
<sup>31</sup>J.P. Perdew and Y. Wang, Phys. Rev. B **33**, 8800 (1986).  
<sup>32</sup>G. Kresse and J. Hafner, Phys. Rev. B **47**, 558 (1993); G. Kresse and J. Furthmüller, Comput. Mater. Sci. **6**, 15 (1996).